In situ electrical characterization of palladium-based single electron transistors made by electromigration technique

L. Arzubiaga, F. Golmar, R. Llopis, F. Casanova, and L. E. Hueso (iD)

COLLECTIONS

Paper published as part of the special topic on Chemical Physics, Energy, Fluids and Plasmas, Materials Science and Mathematical Physics

View Online   Export Citation   CrossMark

ARTICLES YOU MAY BE INTERESTED IN

Metal-nanoparticle single-electron transistors fabricated using electromigration
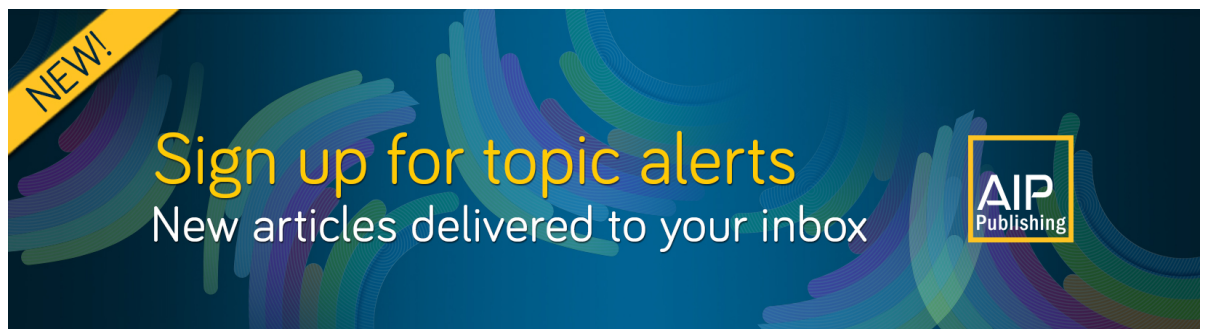Applied Physics Letters **84**, 3154 (2004); https://doi.org/10.1063/1.1695203

Fabrication of metallic electrodes with nanometer separation by electromigration
Applied Physics Letters **75**, 301 (1999); https://doi.org/10.1063/1.124354

Controlled fabrication of nanogaps in ambient environment for molecular electronics
Applied Physics Letters **86**, 043109 (2005); https://doi.org/10.1063/1.1857095

In situ electrical characterization of palladium-based single electron transistors made by electromigration technique

L. Arzubiaga,[1] F. Golmar,[2] R. Llopis,[1] F. Casanova,[1,3] and L. E. Hueso[1,3]

[1]*CIC nanoGUNE, Tolosa Hiribidea 76, 20018 Donostia, San Sebastian, Basque Country, Spain*
[2]*I.N.T.I. – CONICET and ECyT-UNSAM, San Martín, Bs As, Argentina*
[3]*IKERBASQUE, Basque Foundation for Science, 48011 Bilbao, Basque Country, Spain*

We report the fabrication of single electron transistors (SETs) by feedback-controlled electromigration of palladium and palladium-nickel alloy nanowires. We have optimized a gradual electromigration process for obtaining devices consisting of three terminals (source, drain and gate electrodes), which are capacitively coupled to a metallic cluster of nanometric dimensions. This metal nanocluster forms into the inter-electrode channel during the electromigration process and constitutes the active element of each device, acting as a quantum dot that rules the electron flow between source and drain electrodes. The charge transport of the as-fabricated devices shows Coulomb blockade characteristics and the source to drain conductance can be modulated by electrostatic gating. We have thus achieved the fabrication and in situ measurement of palladium-based SETs inside a liquid helium cryostat chamber. © 2014 Author(s). All article content, except where otherwise noted, is licensed under a Creative Commons Attribution 3.0 Unported License. [http://dx.doi.org/10.1063/1.4902170]

The current trend of pursuing an extreme miniaturization of electronic circuits demands appropriate platforms for studying charge transport in systems of reduced dimensions. Single-Electron Transistors (SETs) have attracted much interest in this matter, because they provide the means for observing the circulation of individual electrons in a great variety of nanostructures[1] such as metallic or semiconductor nanoparticles,[2–5] single molecules,[6–8] carbon nanotubes[9–11] or graphene nanoribbons.[12]

The case of SETs constituted by metallic grains is especially interesting. On one hand, it allows probing the influence of quantum confinement in electron-electron correlations and spin-orbit interactions in a given metal. On the other hand, the possibility of alloying different metals offers the opportunity of biasing the type of electronic interactions, for example, by the introduction of ferromagnetism or superconductivity.[2,13] Among the wide variety of metals that could be used as an active element of a SET, palladium could add interesting features to the single electron transport thanks to its peculiar electronic structure. This metal has a fairly strong exchange interaction between electrons, although it has no effective magnetism in the bulk state.[14] Palladium nanoparticles have been reported to display size-dependent magnetism[15] and are thus an attractive element for studying spin-dependent effects in SETs.

The fundamental condition for obtaining a SET is having an active element with dimensions that are low enough to induce the quantum confinement of conduction electrons. This low dimensional element or quantum dot (QD) can be a metallic nanoparticle through which electrons must tunnel to get from source to drain electrodes.

In a SET the QD is directly connected to two terminals (source and drain electrodes) by means of two tunnel junctions with resistance $> R_0$ (where $R_0 = h/2e^2$ is the resistance of a single conductance channel). A third terminal (gate electrode) is used to tune the electrochemical potential in the QD by electrostatic field-effect. When the QD is a metallic nanoparticle of more than a few nanometers, as it is the present case, electrons require an additional amount of energy for tunneling into the

QD. This extra amount of energy, known as the "Coulomb charging energy", allows overcoming the electrostatic repulsion created by the electrons confined in the dot.

The observation of a single electron transport requires E_C to be larger than the thermal energy ($E_C \gg K_B T$, where K_B is the Boltzmann constant and T is temperature). If $E_C \gg K_B T$, an electron tunnels into the QD when the applied source-drain voltage (V_{SD}) provides enough energy to overcome E_C. The devices that meet these conditions show a negligible conductance when a low source-drain voltage (V_{SD}) is applied, which is a situation known as Coulomb blockade. Thus, the QD acts as a bottleneck in the circuit where electrons are forced to pass one at a time.[1]

There are interesting examples in literature describing the fabrication of SETs based on metallic QDs. Such techniques comprehend one or more steps for creating nanoelectrodes (employing lithography or alternative techniques), followed by the addition of metallic nanoparticles obtained by chemical or physical methods.[16–18] The use of electromigration for the fabrication of SETs is quite extended, as it has enabled the fabrication of transistors with channel lengths as small as 1 nm.[3,6–8]

Electromigration consists on passing a high electrical current density through a metallic wire of nanometric cross-section, until it breaks by electrical stress. Metallic QDs can then be placed and electrically contacted in the gap between the obtained electrodes. The combination of certain experimental conditions during the electromigration process and the intrinsic properties of the nanowire material can favor the simultaneous formation of metallic nanoclusters or nanoparticles at the breaking point. The newly formed metallic nanoparticles have the advantage of being already embedded in the gap between two electrodes. Hence, the as-fabricated device would be ready for electrical characterization without further manipulation.

The formation of SETs with metallic quantum dots as a consequence of electromigration has already been reported.[7,19] These devices have generally been regarded as undesired by-products when the aim was obtaining single molecule transistors (SMTs). We would like to show that the spontaneous formation of SETs during electromigration could also be used to our advantage.

We used electron-beam lithography for defining palladium devices on top of p-doped silicon chips coated with 150 nm of thermally grown silicon oxide (SiO_2). The lithography was carried out on a double layer polymethyl metacrylate (PMMA) resist system spun onto the thermal SiO_2 surface, followed by metal deposition by magnetron sputtering and lift-off in acetone. We fabricated devices with 99.99% purity Pd.

Each device consisted of a palladium nanowire (around 300 nm long, 25 nm thick and 65 nm wide) terminated with a pair of macroscopic electrodes for electrical contact. The as-fabricated palladium devices were cleaned with acetone and isopropanol, followed by 10 seconds of oxygen plasma, before placing them in a liquid helium cryostat.

All the electromigration and electrical characterization experiments were carried out at 1.8K inside a liquid He cryostat (with 10 mTorr He atmosphere). A home-made LabView program controlled the electromigration process with the aid of an appropriate feedback algorithm. The nanowires were gradually broken by electromigration. The strategy consisted on applying series of increasing voltage ramps and limiting the extent to which the electromigration took place in each ramp. This was done by continuously monitoring the conductance (G) measured across the device and limiting the amount it changed in the last measured 40 data points. Fig. 1 shows the conductance of a device as it evolved in a typical electromigration process. At the beginning of each voltage ramp the conductance of the device decreased slightly, due to the increase of electron scattering events as the circulating current got higher. The observation of a sudden decrease of conductance marked the starting point of electromigration. We will refer to the values of voltage and current at the onset of electromigration as the critical voltage (V_C) and critical current (I_C), respectively. Typically, we limited the decrease of conductance to a 1.5% in the last measured 40 data points, after which the applied voltage was reset to zero and a relaxation time of 5 seconds was allowed. These conditions ensured that the electromigration in the nanowire occurred only partially in each voltage ramp. As the gradual breaking process of the nanowires was carried out, the value of V_C decreased. When the onset of electromigration took place at V_C values lower than about 500 mV, we allowed the nanowire to electromigrate beyond the previously set limits. During the final voltage ramps the nanowires suffered a sudden and major break (which could bring the device resistance up to several KΩ). Afterwards, the evolution of the conductance entered a different regime in which sudden jumps of random character were often observed.
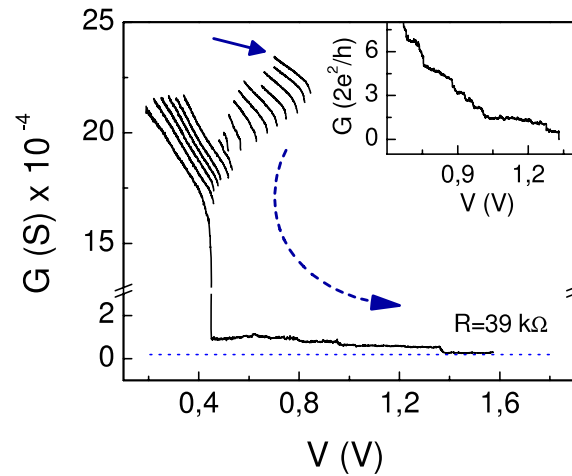
FIG. 1. Evolution of the device conductance (G) during the electromigration process of a palladium nanowire. A series of increasing voltage (V) ramps are applied while the decrease of G in each V ramp is limited to a 1.5%. The solid arrow indicates the starting point of the first V ramp, while the dashed arrow shows the order of the successive V ramps throughout the process. The gradual decrease of G indicates that the cross-section of the nanowire is decreased after each V ramp. After the nanowire suffers a major break (observed as a sharp jump in G) it becomes unstable. G evolves in random jumps until a target G value (corresponding to a device resistance of around 40 kΩ, indicated by a dotted line) is reached. Inset: Evolution of the conductance (G) in units of quantized conductance ($G_0 = 2e^2/h$) in the last stage of the electromigration for a similar nanowire. The appearance of quantized conductance steps indicates the formation of a narrow constriction before the failure of the nanowire.

The applied voltage was steadily increased until a target conductance value was reached (typically corresponding to a device resistance of around 40 KΩ), after which the voltage was reset to zero and the process was finished. At this point, the low bias resistance of the devices had a value in the order of 1 to 100 MΩ (measured at 20 mV and 1.8 K) and the measured current versus voltage curves became non-linear.

During an electromigration process the nanowires develop constrictions that grow gradually throughout several voltage ramps until they finally break.[20] This is consistent with the steady decrease of G measured during the first few voltage ramps of the process (Fig. 1). As regards the more random evolution and the sudden jumps of G observed in the last stage of the process, they are generally attributed to rearrangements of the metal grains. We could occasionally observe the conductance decreasing in quantized steps in this last stage. This quantization indicated the formation of a constriction with a few conductance channels just before the complete breakdown of the nanowire.

The source-drain current (I_{SD}) versus voltage (V_{SD}) curves of the electromigrated devices were non-linear, with a plateau of almost negligible source-drain current near the zero bias region. On the other hand, most of the obtained devices showed a periodic modulation of the described transport features as a function of the applied gate potential (V_G). This last observation confirmed that after the electromigration of the nanowires, the devices had indeed transformed into SETs in which the current passed through a QD. The modulation with V_G occurs because the electrostatic energy of the QD is shifted with respect to the Fermi energy (E_F) of the source and drain electrodes by field effect.

The effect of V_G is more easily analyzed in the differential conductance curves (dI/dV), which are obtained by calculating the derivative of the recorded I_{SD} vs V_{SD} traces. The circulation of single electrons into or out of the QD is marked by peaks in the dI/dV. These peaks appear at different V_{SD} values depending on the applied V_G. We calculated the dI/dV curves for a range of gate voltages and we plotted them as a function of V_{SD} and V_G. The resultant graphs, commonly known as "stability diagrams", constituted a conductance-map of the devices. Some of our devices showed stability diagrams with the characteristic pattern of a SET, in which we observed periodic diamond-shaped regions of almost negligible conductance (Fig. 2).

The average number of electrons inside the QD is fixed in each of the so-called Coulomb diamonds. Hence, contiguous diamonds represent charge states that differ by just one electron. The
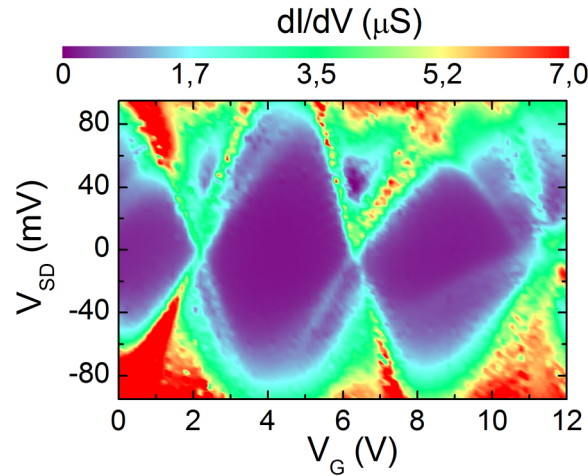
FIG. 2. Stability diagram of palladium SET obtained by electromigration. Plotting the derivative of the drain current (dI/dV) as a function of bias voltage (V_{SD}) and gate voltage (V_G) results in a pattern of diamond-shaped regions of almost negligible conductance. These conductance features are a signature of the Coulomb blockade regime and they indicate the transformation of the palladium nanowires into QDs after electromigration.

dimensions and shape of the diagram can be used to extract information about the studied systems.[2,3,5,7] The longest dimension of the Coulomb diamonds in the V_{SD} axis is related to the charging energy ($\Delta V_{SD} = 2E_C/e$). The charging energy can be written as $E_C = e^2/2C$, where C is the total capacitance of the quantum dot. The capacitance is related to the size of the QD and therefore, we can extract information about its approximate dimensions using a simple model, such as that of a conducting sphere into a dielectric environment. In this case we can use the expression for the self-capacitance of a sphere $C = 2\varepsilon d$, where ε is the absolute permittivity of the dielectric media and d is the diameter of the conducting QD. According to these expressions, we extracted the following values from the left (1) and right (2) diamonds, in the stability diagram of Fig. 2: E_C (1) = 6.47 x 10^{-21} J and E_C (2) = 4.22 x 10^{-21} J for the charging energy; C (1) = 1.98 x 10^{-18} F and C (2) = 3.04 x 10^{-18} F for the total capacitance; d (1) = 9.1 nm and d (2) = 14 nm for the approximate diameter of the QD (assuming a spherical shape and the value $\varepsilon = 3.45$ x 10^{-11} F/m for the silicon dioxide gate dielectric, on top of which the QD was located). It is not unusual to observe differences in the size of the Coulomb diamonds, as in the present case on Fig 2. They are a consequence of the background charge in the silicon oxide surrounding the QD, which may vary when applying the gate potential, as the charge traps in the oxide get or release electrons. The biggest dimension of the Coulomb diamond in the V_G axis is related to the gate capacitance ($\Delta V_G = e/C_G$), whereas the capacitance between the quantum dot and the drain (source) electrodes can be extracted from the positive (negative) slope of the diamonds ($\alpha^+ = C_G/(C_G+C_D)$ and $\alpha^- = -(C_G/C_S)$). Based on these expressions, we extracted the following values from the slopes of the diamonds in Fig. 2: $C_G = 3.72$ x 10^{-20} F, $C_S = 6.48$ x 10^{-19} F and $C_D = 1.29$ x 10^{-18} F, which agree fairly well with literature. As expected, the capacitance with the gate electrode was one or two orders of magnitude smaller than with the source and drain electrodes. This was consistent with the approximate distances from the QD to the gate (150 nm, the thickness of gate oxide), source and drain (tunnel barriers of a few nm).[2,3,5] Similarly, the periodicity of the diamonds in the V_G axis is related to the gate coupling. Using the expression $\Delta V_G = E_C/e\beta$ we can extract an approximate value of 0.019 for the gate coupling (β). This number is close to the value expected for a SiO_2 gate dielectric of 150 nm thickness.[5]

We must note that although approximately a 90% of our devices showed Coulomb blockade, only around a 15% displayed clearly distinguishable Coulomb diamonds, consistent with the charge transport through a single quantum dot. The formation of several nanoparticles conducting in parallel was often observed, giving as a result a pattern of superposed diamonds in the stability diagram that was not appropriate for extracting useful information about the QDs.[5]
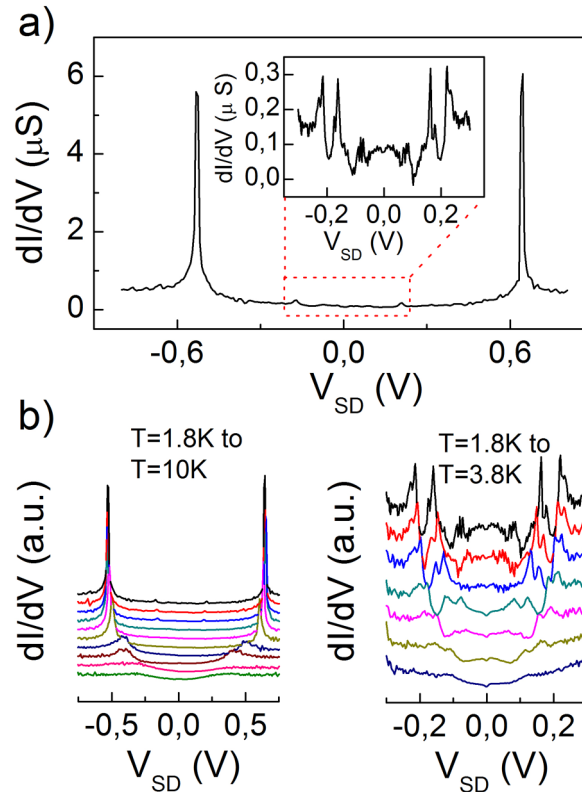
FIG. 3. Unusual conductance features in palladium devices. Unusual features in the form of symmetric and sharp resonance peaks appeared in a number of palladium devices. Inelastic tunneling processes involving spontaneous magnetization of the atomic-sized palladium structures have been proposed as a possible explanation. a) Detail of the resonance peaks appearing consistently into two clusters, around $V_{SD} = 0.5$ and below $V_{SD} = 0.3$ V (as shown in the inset). b) Temperature dependence in the position and intensity of the peaks at high bias (left) and low bias (right).

More unusual conductance features appeared in some devices, such as the sharp resonance peaks shown in Fig. 3. The observed conductance features appeared in two different sets, which were symmetrically located with respect to V_{SD}. The first set appeared at low bias and comprised a cluster of small peaks of different sizes. The other one consisted of two bigger peaks (with several µS intensity) located around $V_{SD} = 0.4$ V. Same as reported in literature,[14] both the intensity and position of these peaks depended on temperature. They shifted to lower V_{SD} values and decreased in size when increasing the temperature. The low-bias features became imperceptible at a temperature of about 4K, while the high-bias peaks were visible up to 10K. However, neither of these features was affected by applied magnetic fields or V_G. The origin of these peaks remains still unclear, although the authors of the cited work ruled out several physical mechanisms after exhaustive experimental and theoretical studies. Inelastic tunneling processes involving spontaneous magnetization were finally proposed as a possible explanation. This hypothesis is consistent with the onset of ferromagnetism predicted for palladium nanoparticles and atomic-sized contacts,[21,22] although further experiments would be needed for a full understanding.

These sharp resonances had only been observed in electromigrated palladium devices, according to literature and consequently, they had been attributed to an intrinsic phenomenon particular only to this metal. Interestingly, we also observed similar features in a nickel device (see Figure 4), which pointed toward the fact that such peculiarities in the conductance could perhaps be attributed to the formation of specific nanostructures, instead of to the inherent properties of palladium itself. We note the resemblance of the observed differential conductance peaks with the ones arising from the Van Hove Singularities (VHS) in the DOS of a one dimensional system, such as a carbon nanotube. The
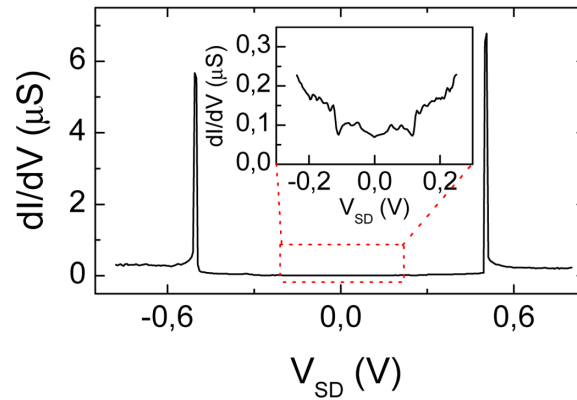
FIG. 4. Unusual conductance features in nickel devices. Sharp resonance peaks in the differential conductance curve of an electromigrated nickel device at T=1.8K. The resemblance of these features to the peaks observed in several palladium devices seems to indicate that they belong to the same type of resonance or excitation.

VHS would account for the sharp peaks presented in the differential conductance curves of Figures 3 and 4.

In the case of the nickel device of Figure 4 the peaks at low bias are not so well defined and intense as those observed in the palladium device in Figure 3. Their shape and intensity are closer to the traces recorded at higher temperatures in the palladium devices (see the graph on the right in Figure 3(b)). With regard to the peaks at high bias, we observe that they are sharper than in the case of palladium. The shape of the peaks observed for nickel devices is fairly asymmetric, since they show a very abrupt drop when decreasing bias, while the decay is more gradual for increasing bias. Qualitatively speaking, this detail resembles again the typical profile of the VHS.

Preliminary tests of electromigration with palladium alloy devices ($Pd_{0.5}Ni_{0.5}$) were also carried out following the same strategy as explained for palladium devices. Again, we observed Coulomb diamonds, confirming that our method was also valid when alloying the palladium with nickel up to a 50 atomic %. This opened up the possibility of fabricating and studying a series of alloyed devices covering the whole range from 0 to 50 atomic % nickel content. We would expect Pd to play a role in the magnetic properties, due its strong exchange interactions. However, studying electronic correlations at this level implies working at dilution-refrigerator temperatures for enabling the observation of the individual electronic energy levels of the metallic grains,[2] which for the time being has been impossible for us.

In conclusion, we have obtained devices working in the single electron transport regime by performing feedback-controlled electromigration of palladium nanowires. Breaking palladium nanowires at low temperature by a gradual electromigration process resulted in the simultaneous formation of closely separated nanoelectrode pairs (source and drain) and metallic quantum dots. The newly formed quantum dots showed an adequate coupling to source, drain and back-gate electrodes for exploring single electron physics. The formation and subsequent measurement of these nanostructures inside a virtually inert atmosphere of a He cryostat allowed skipping additional fabrication steps. Additionally, we have shown that the fabrication method can be extended to palladium-based alloys, such as $Pd_{0.5}Ni_{0.5}$, which offer the opportunity of studying magnetic effects. This result suggests that Pd could be used as a medium for driving the formation of SETs with small amounts of other elements, which is an attractive prospect. Precisely, one of the difficulties of obtaining SETs with magnetic nanoparticles is that they tend to oxidize, since metallic nanoparticles have enhanced reactivity when compared to bulk metals. Hence, the proposed approach, in which the samples are fabricated and measured in situ, would be most convenient for studying non - noble metals.

[1] C. W. J. Beenakker, Phys. Rev. B **44**, 1646 (1991).

[2] J. V. Delft and D. C. Ralph, Phys. Rep. **345**, 61 (2001).

[3] F. Kuemmeth, K. I. Bolotin, S. F. Shi, and D. C. Ralph, Nano Letters **8**, 4506 (2008).

[4] S. J. Shin, C. S. Jung, B. J. Park, T. K. Yoon, J. J. Lee, S. J. Kim, J. B. Choi, Y. Takahashi, and D. G. Hasko, Appl. Phys. Lett. **97**, 103101 (2010).

[5] E. A. Osorio, T. Bjørnholm, J. M. Lehn, M. Ruben, and H. S. J. van der Zant, J. Phys: Concens Matter. **20**, 374121 (2008).

[6] J. Park, A. N. Pasupathy, J. I. Goldsmith, C. Chang, Y. Yaish, J. R. Petta, M. Rinkoski, J. P. Sethna, H. D. Abruña, P. L. McEuen, and D. C. Ralph, Nature **417**, 722 (2002).

[7] D. R. Ward, G. D. Scott, Z. K. Keane, N. J. Halas, and D. Natelson, J. Phys.: Condens. Matter **20**, 374118 (2008).

[8] R. Vincent, S. Klyatskaya, M. Ruben, W. Wernsdorfer, and F. Balestro, Nature **488**, 357 (2012).

[9] S. Sahoo, T. Kontos, J. Furer, C. Hoffmann, M. Graber, and A. Cottet, Nat. Phys. **1**, 99 (2005).

[10] L. E. Hueso, G. Burnell, J. L. Prieto, L. Granja, C. Bell, D. J. Kang, M. Chhowalla, S. N. Cha, J. E. Jang, G. A. J. Amaratunga, and N. D. Mathur, Appl. Phys. Lett. **88**, 083120 (2006).

[11] P. Jarillo-Herrero, J. A. van Dam, and L. P. Kouwenhoven, Nature **439**, 953 (2006).

[12] F. Prins, A. Barreiro, J. W. Ruitenberg, J. S. Seldenthuis, N. Aliaga-Alcalde, L. M. K. Vandersypen, and H. S. J. van der Zant, Nano Lett. **11**, 4607 (2011).

[13] P. Seneor, A. Bernand-Mantel, and F. Petroff, J., Phys.: Condens. Matter **19**, 165222 (2007).

[14] G. D. Scott, J. J. Palacios, and D. Natelson, ACS Nano **4**, 2831 (2010).

[15] T. Taniyama, E. Ohta, and T. Sato, Europhys. Lett. **38**, 195 (1997).

[16] J. F. Dayen, V. Faramarzi, M. Pauly, N. T. Kemp, M. Barbero, B. P. Pichon, H. Majjad, S. Begin-Colin, and B. Doudin, Nanotechnology **21**, 335303 (2010).

[17] K. I. Bolotin, F. Kuemmeth, A. N. Pasupathy, and D. C. Ralph, Appl. Phys. Lett. **84**, 3155 (2004).

[18] J. E. Grose, A. N. Pasupathy, and D. C. Ralph, Phys. Rev. B **71**, 035306 (2005).

[19] R. Sordan, K. Balasubramanian, M. Burghard, and K. Kern, Phys. Rev. Lett. **87**, 013106 (2005).

[20] K. I. Bolotin, F. Kuemmeth, A. N. Pasupathy, and D. C. Ralph, Nano Lett. **6**, 123 (2006).

[21] K. Lee, Phys. Rev. B **58**, 2391 (1998).

[22] A. Delin, E. Tosatti, and R. Weht, Phys. Rev. Lett. **92**, 057201 (2004).